

Extracting Rayleigh Waves from Noise Using a Differential Optical Interferometer

A. M. Shokry, J. A. Gilbert

Consortium for Holography, Applied Mechanics and Photonics (CHAMP), University of Alabama at Huntsville, Huntsville, AL 35899, USA.

Abstract. This article introduces a new strategy for extracting Rayleigh waves from a noisy environment using a differential optical interferometer (DOI). The DOI consists of a bidirectional coupler; one arm, positioned over a test specimen, senses an acoustic signal immersed in noise while the other arm, positioned over an acoustic isolator, senses the noise alone. Analytical arguments show that when the coupler is designed properly, the phase shifts between the signals returning to a photodetector produce an intensity modulation that is directly proportional to the pure acoustic signal. The analysis is verified when the DOI is used to track the surface displacement of a piezoelectric transducer. Then, random noise is introduced into an aluminum test specimen using a motor equipped with a rotating eccentric cam. The DOI is used to subtract the relatively high-amplitude but low-frequency mechanical vibrations of the test surface from a combined signal that includes the desired Rayleigh wave. Finally, an experimental configuration is demonstrated which allows an acoustic signal to be extracted from noise of a similar frequency.

Introduction

A viable and widespread approach for nondestructive evaluation is to intentionally generate elastic waves in a controlled manner; the ultrasonic radiation is measured by using a transducer in an attempt to establish material characteristics or to identify inherent flaws. In a homogeneous, isotropic, and unbounded elastic medium, the elastic waves propagate as either longitudinal (pressure) or transverse (equivoluminal, distortional, shear) waves. When there is a bounding surface, Rayleigh (surface or R) waves [1] may also occur. Because R-waves propagate on the free surface over larger distances than those associated with longitudinal or shear waves, they are ideal for detecting surface and subsurface flaws. The R-wave causes the individual particles in the body to move in an elliptical motion; the displacements and the corresponding energy content of the wave decay with the depth measured from the free surface. For a given material, the R-wave travels at a constant speed and the depth of penetration is approximately a wavelength.

¹ Symbols and definitions in this article: n_i , index of refraction; I , intensity from the DOI; I_i intensity of light beams; I_0 , intensity to the DOI; I_R , intensity of reflected wave; I_T , intensity of transmitted wave; J_{ij} , optical interference terms; R , reflectivity; T , transmissibility; λ , wavelength; ϕ_i , phase.

These properties make it possible to apply time domain reflectometry and spectroscopic analysis to determine flaw location and depth.

Unfortunately, however, both the amplitude and energy associated with an R-wave are relatively small compared to the strong and broadband acoustic responses produced by sources of mechanical noise. The noise limits practical applications in which tests must be conducted under field conditions. Simply put, the ability to identify or eliminate noise is one of the most outstanding problems facing the ultrasonics community today.

The solution to the problem lies in improving the performance characteristics of existing sensors or uncovering new and better testing methods. To date, it has been impossible to satisfy all of the requirements for an ideal ultrasonic transducer and/or measurement system [2]. The most widely available lead zirconium titanate (PZT or piezoelectric) transducers, for example, are limited by the fact that the frequency bands of these devices are relatively narrow [3]. They require direct contact with the specimen, are highly sensitive to background noise, and the measurement systems are affected by electromagnetic fields. Some of these problems have been eliminated by using semicrystalline polymers such as polyvinylidene fluoride (PDVF) [4] or by relying on optical methods [5–9]. However, all of the existing ultrasonic detection systems require a high signal-to-noise ratio and/or rely on filtering the acoustic signal from the noise. In general, increasing the signal-to-noise ratio requires careful control of the operating environment, whereas filtering necessitates that the signal be at a frequency that is different from that of the noise.

This paper introduces a new strategy for extracting acoustic signals from a noisy environment using a differential optical interferometer (DOI). Results show that this noncontacting, fiber optic transducer can be configured to detect R-waves in the presence of noise even when the noise is at a level that is substantially greater than that of the acoustic signal. Under certain test conditions, an acoustic signal can be extracted from noise of a similar frequency.

Optical Configuration of the DOI

As shown in Fig. 1, the DOI consists of a bidirectional coupler constructed using single mode optical fibers. Laser light, launched into the input arm, is divided equally by the coupler into the two output arms labeled #1 and #2. Arm #1 is positioned normal to the test surface, while arm #2 is positioned normal to an acoustic isolator that is designed to eliminate the desired acoustic signal. In this configuration, arm #1 detects both the noise and the acoustic signal from the surface while arm #2 picks up only the noise from the isolator. By employing graded index (GRIN) lenses on the fiber tips and reflective foil stickers on both test surfaces, most of the impinging light is reflected back into the fibers. However, a small portion of the light is internally reflected by the glass/air interface at the fiber tips. These backreflections interfere with the light coming from the surface and the acoustic isolator. By appropriately adjusting the intensities and phases of the light passing through the DOI, a pure acoustic signal can be obtained.

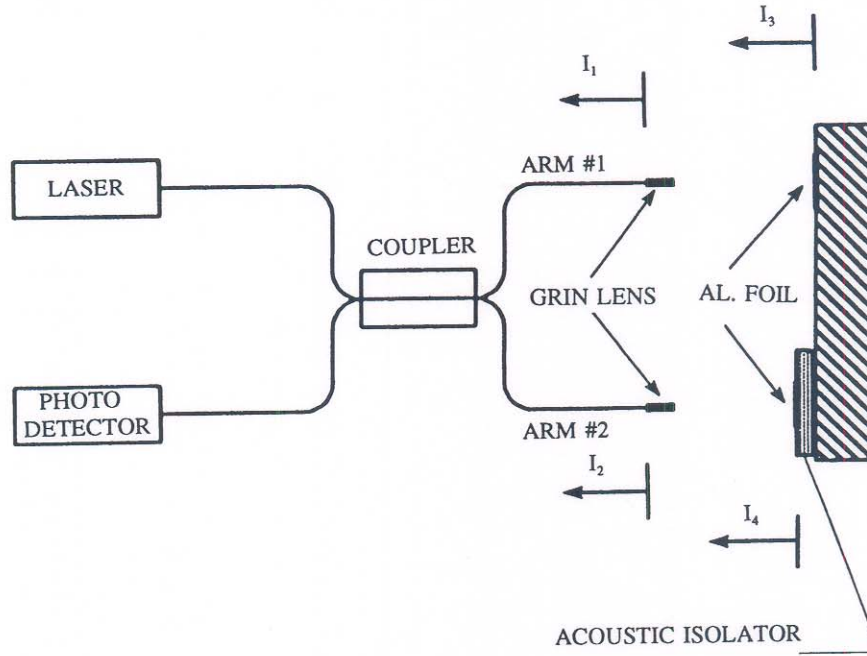


Fig. 1. Schematic diagram of the differential optical interferometer (DOI).

Theoretical Analysis of the DOI

Referring to Fig. 1, the total intensity emerging from the DOI is given by:

$$I = \frac{1}{2}[(I_1 + I_2 + I_3 + I_4) + (J_{12} + J_{13} + J_{14} + J_{23} + J_{24} + J_{34})] \quad (1)$$

where the terms J_{ij} represent the interference that takes place between the i th and j th beams such that

$$J_{ij} = 2\sqrt{I_i I_j} \cos(\phi_i - \phi_j) \quad i \neq j. \quad (2)$$

The right-hand side of Eq. (1) is divided by two because one-half of the return signal is lost when it passes back through the coupler to the photodetector.

Equation (2) shows that the interference terms depend on the phase differences ($\phi_i - \phi_j$) and the light intensities of the two beams in question. In the DOI, ϕ_1 and ϕ_2 are modulated by stresses introduced into fiber arms #1 and #2, respectively. Assuming that light is scattered back into arm #1 from the test surface, ϕ_3 is modulated by a combination of the noise (mechanical vibration, etc.) and the acoustic signal (R-wave) in the specimen. Provided that the acoustic isolator dampens out the R-wave, ϕ_4 is modulated by the noise alone.

When the fiber arms are adjusted so that the difference in path lengths produces a relative phase change of π and the coupler divides the input light equally between the

output legs, the output from the DOI is given by

$$I = \frac{1}{2}[I_3 + I_4] + \sqrt{I_3 I_4} \cos(\phi_3 - \phi_4). \quad (3)$$

If the noise at both sensing locations is the same, the phase difference $(\phi_3 - \phi_4)$ is a measure of the pure acoustic signal.

Performance of the DOI

Assuming the input intensity to be I_0 , the light traveling to the exit end of each leg is $I_0/2$. The intensity of the backreflections, I_1 and I_2 , depend on the reflectivity R of the surfaces at the fiber tips. Theoretically,

$$R = \left[\frac{n_1 - n_2}{n_1 + n_2} \right]^2, \quad (4)$$

where n_1 and n_2 are the indices of refraction of the fiber core and the surrounding medium, respectively. For $n_1 = 1.46$ (fused silica) and $n_2 = 1.0$ (air),

$$R = \left[\frac{0.46}{2.46} \right]^2 = 0.035 \quad (5)$$

and

$$I_1 = I_2 = I_R = 0.035 \frac{I_0}{2} = 0.0175 I_0. \quad (6)$$

Because the reflectivity is related to the transmissibility T by

$$R + T = 1.0, \quad (7)$$

the intensity of the transmitted beam is

$$I_T = 0.965 \frac{I_0}{2} = 0.4825 I_0. \quad (8)$$

The efficiency of the system is increased when the light reflected back from the surface (I_3) and from the acoustic isolator (I_4) are increased. By using GRIN lenses and applying reflective stickers onto the illuminated surfaces, it is theoretically possible to increase the intensities of the beams returning through the interface to 95% of those transmitted through the lens. Considering Eq. (8),

$$I_3 = I_4 = 0.95 I_T = 0.4584 I_0, \quad (9)$$

and Eq. (3) becomes

$$I = [0.4584 + 0.4584 \cos(\phi_3 - \phi_4)] I_0. \quad (10)$$

Equation (10) demonstrates that 92% of the laser power is utilized and modulation occurs over 100% of the output intensity.

The relative phase difference in the arms is sensitive to mechanical and thermal disturbances, and the coupler may be affected by polarization fading. These problems can be reduced by employing a phase lock system and by using polarization-preserving fibers. However, the tests to be described demonstrate that satisfactory results can be obtained without taking these steps. One reason for this is that the reflectances from the ends of the fiber legs are so small that they can be neglected compared to the signals reflected from the stickers.

To be self-compensated against temperature, both arms of the DOI must be of the same length and operate under the same environmental conditions. In addition, the two air gaps between the fiber tips and the test surfaces must be equal and have the same index of refraction.

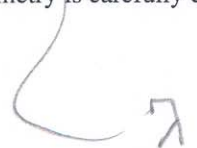
Isolator and Optrodes

The DOI relies on the fact that the acoustic isolator responds to the noise but not to the ultrasonic signal; that is, the isolator must be capable of completely absorbing an R-wave. The attenuation of the wave depends on the material properties and the interfaces between the different materials utilized in the design. While testing aluminum specimens, it was experimentally determined that the impedance, absorption, and rigidity requirements for a 3.0-mm-diameter acoustic isolator could be met by mounting a 0.5-mm-thick layer of polystyrene to the test surface using a 1.0-mm-thick layer of hot glue. Aluminum foil was selected for the reflective stickers because there is no change in acoustic impedance between the specimen and the aluminum foil. An added advantage of placing the aluminum foil on the acoustic isolator was that an abrupt change in the acoustic impedance occurred between the polystyrene and the sticker itself. This further improved the efficiency of the isolator.

A schematic representation of the test apparatus is illustrated in Fig. 2. Each fiber tip is housed in a 3.3-mm-diameter sleeve that allows it to be positioned relative to a 1.8-mm-diameter, quarter-pitch GRIN lens. The holders were mounted in micropositioners to facilitate the adjustment of the optrodes relative to the test surfaces.

It was found that a convergent illumination was required to ensure that the size of the illuminated spot was small compared to the acoustic wavelength of the R-wave. Calculations showed that, for an R-wave generated at a frequency of 2.25 MHz, the spot size had to be less than 1.3 mm. A typical stand-off distance measured from the optrode to the surface was 2 mm.

The center-to-center distance between the optrodes was found to place a restriction on the frequency range over which noise could be eliminated. In general, the spacing between the optrodes must be relatively small with respect to the wavelength of the noise so that the noise is the same in both sensing locations. Assuming that the noise is characterized by a cosine wave of length λ , and that it is desired to eliminate 90% of the noise, the optrodes must be positioned at a center-to-center distance of approximately 0.03λ . Since the smallest center-to-center distance that can be achieved with the present optrode design is 5 mm, the upper threshold on noise removal is 37.7 kHz. However, higher frequency noise (on the order of MHz) may be removed provided that the testing geometry is carefully chosen. This approach is illustrated later in the paper.



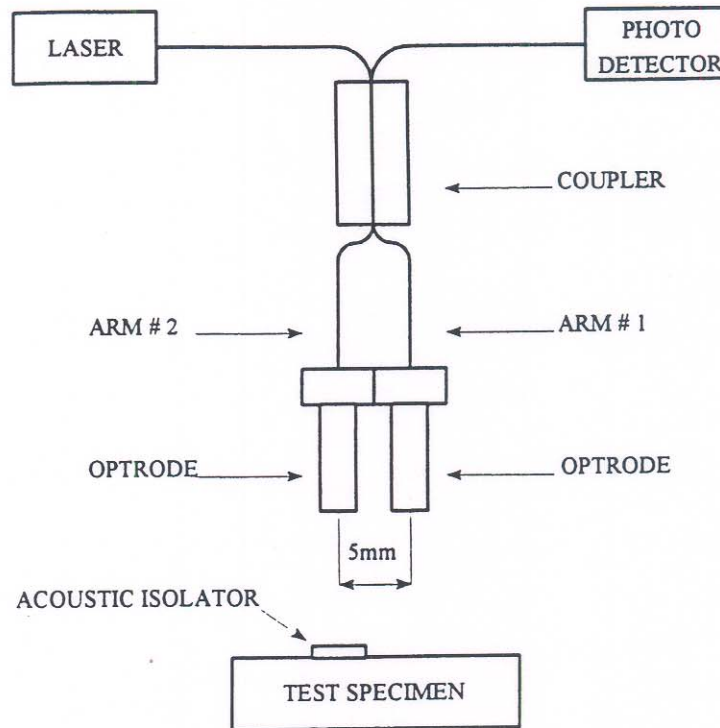


Fig. 2. A schematic representation of the test apparatus.

System Evaluation and Proof of Principle

The basic operating principle of the DOI was tested by launching a 150-mw laser (Spectra Physics, Model No. 265, krypton with $\lambda = 647$ nm) into the input arm of a single-mode fiber optic coupler (Corning). The coupler was made from nonpolarization-preserving fiber having a core diameter of $4\text{ }\mu\text{m}$; the fiber cladding had an outer diameter of $125\text{ }\mu\text{m}$, and the numerical aperture was 0.14. The return arm of the coupler was connected to a photodetector and amplifier (Opto Acoustic Sensors, Inc.) capable of detecting signals with frequencies ranging from 0 to 35 MHz. The output signal was fed to a digital storage oscilloscope (Lecroy).

The two output arms were used to monitor the active surface of a 12.7-mm-diameter piezoelectric transducer (Harisonic, Model No. 13-0008P) having a resonant frequency of 0.5 MHz. The transducer was excited using a wide-band signal generator. As described in the preceding section, both arms of the DOI were fitted with quarter-pitch GRIN lenses; the lenses were aligned normal to the surface, and reflective foil stickers were used to increase the reflectivity.

The upper trace in Fig. 3 illustrates the output from the signal generator when no laser light is launched into the DOI. In this case, all of the electronics (photodetector, laser power supply, oscilloscope, etc.) are switched on. Because this noise is less than 10 mV,

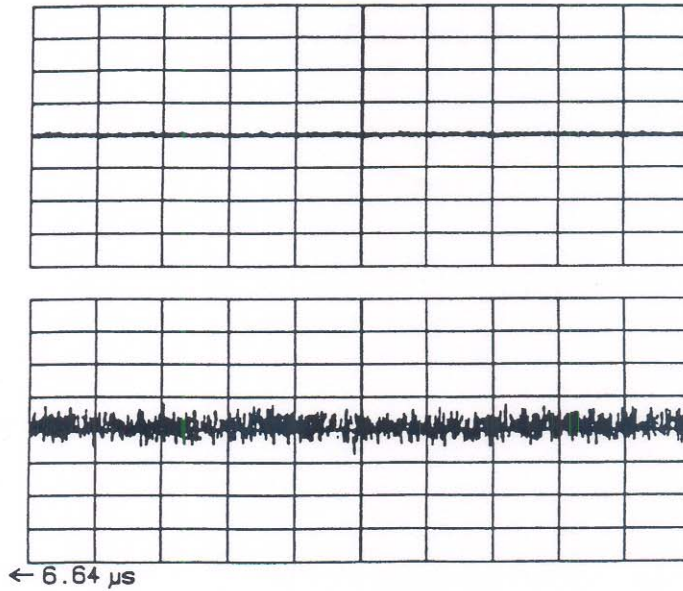


Fig. 3. Noise from the pulse generator (upper trace) and the photodetector (lower trace). The vertical gain on each trace is 50 mV/div; the horizontal gain on each trace is 2 μ s/div.

it can be neglected. The lower trace, on the other hand, represents the dark noise of the photodetector. Because the noise is on the order of 50 mV with a frequency of 30 MHz, it must be taken into consideration when making comparisons between figures and results. The dark noise in the photodetector remained constant when the transducer was excited, indicating that no electromagnetic interference occurred between the electronics and the optics.

In the first test conducted with laser illumination, one of the arms of the DOI was positioned over the center of the transducer while the other was slightly offset. In this configuration, the displacement under each arm is different but the frequency of the signals is the same. The upper trace in Fig. 4 corresponds to the output of the signal generator adjusted to produce a signal at the transducer's resonant frequency of 0.5 MHz, while the lower trace corresponds to the output from the DOI. The latter corresponds to the difference in the signals detected by the two arms and, as such, represents the movement of the transducer's surface. The constant dark noise inherent in the photodetector is superimposed on the signal; slight instabilities in the baseline were attributed to the failure of the coupler to split the light between the fibers equally, and to the differences in polarizations and path lengths that took place in the fibers.

A second test was conducted with the arms of the DOI positioned symmetrically over the piezoelectric transducer. The lower trace of Fig. 5 shows that, in this case, the amplitude of the output signal reduces to the level of the dark noise (see Fig. 3).

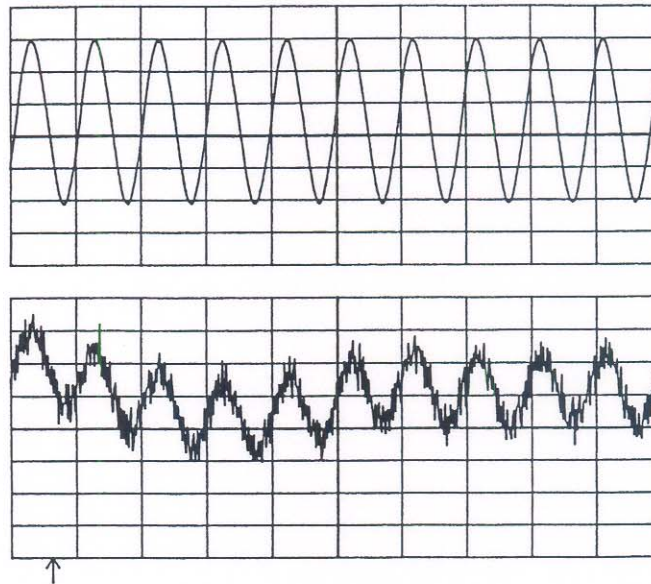


Fig. 4. Results obtained by placing a DOI with its arms positioned asymmetrically over a piezoelectric transducer. The upper trace corresponds to a generating signal of 500 kHz while the lower trace shows the signal detected by the asymmetric DOI. The vertical gains on the upper and lower traces are 200 and 50 mV/div, respectively; the horizontal gain on each trace is 2 μ s/div.

Extraction of an R-Wave from Random Noise

When conducting ultrasonic tests, it is preferable not to have devices such as electric motors or other machinery operating nearby. In the past, when such sources could not be avoided, the threshold level of the signal had to be increased to the point at which it exceeded the noise level, or, alternately, the signal had to be isolated by selecting an appropriate bandpass filter.

Figure 6 shows a test setup in which a DOI is used to acquire an R-wave in the presence of random noise. Arm #1 is positioned directly over a reflective foil sticker placed on the surface of a 406-mm-long \times 25.4-mm-wide \times 2.54-mm-thick aluminum specimen while arm #2 is positioned over a second sticker on an acoustic isolator mounted on the test surface. Random noise is generated by placing an electric motor equipped with a rotating eccentric cam on the same table that supports the specimen. The resulting vibrations are transferred to the specimen through the support posts.

The arms of the DOI are spaced 14 mm apart and are intentionally located at the same distances from the posts and positioned symmetrically over the width of the specimen so that the vibrations created by the motor have the same phase at both arms. Only in this configuration can the noise be completely removed independent of frequency. Otherwise, for the 14-mm spacing, the upper bound for 90% noise removal would be only 13.5 kHz.

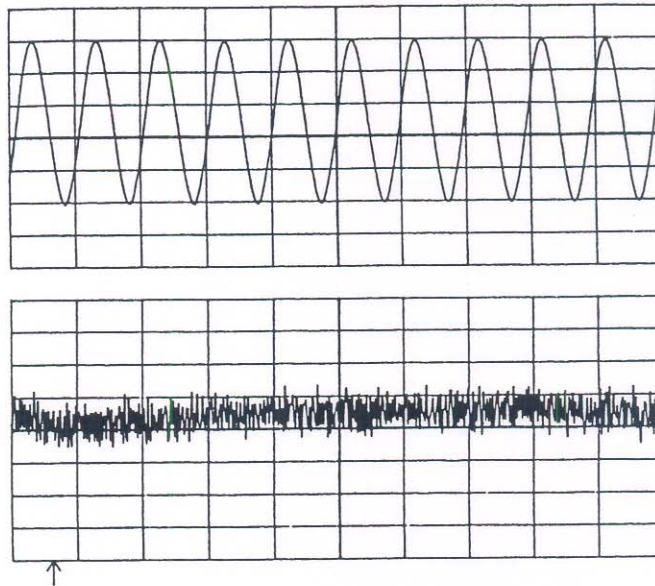


Fig. 5. Results obtained by placing a DOI with its arms positioned symmetrically over a piezoelectric transducer. The upper trace corresponds to the generating signal of 500 kHz while the lower trace shows the signal detected by the symmetrical DOI. The vertical gains on the upper and lower traces are 200 and 50 mV/div, respectively; the horizontal gain on each trace is 2 μ s/div.

The 0.5-MHz piezoelectric transducer, used to illustrate the proof of principle and labeled as #2, is attached to the lower surface of the test specimen to verify that the noise created by the motor is actually transmitted to the specimen. An R-wave is generated on the upper surface of the specimen using a 2.25-MHz R-wave transducer labeled as #1. This transducer is positioned along the center line of the specimen at a distance of 24.5 mm from both arms of the DOI. It should be noted that the R-wave speed in the aluminum specimen is 2.89 mm/ μ s.

The upper trace in Fig. 7 shows the response of the 0.5-MHz transducer while the lower trace shows the output from the DOI. A distinct R-wave appears at the expected arrival time of 18.5 μ s, which includes the 10- μ s delay in the transducer and 8.5 μ s for the time-of-flight. When arm #2 was removed and immersed in an index matching fluid, an R-wave of approximately the same amplitude could be observed, but the baseline moved so erratically that it was impossible to capture the wave in real time without substantially reducing the vertical gain of the oscilloscope.

It should be noted that the signal in the upper trace of Fig. 7 is displayed without amplification while the signal from the DOI is amplified 1000 times. It is apparent from the upper trace that substantial noise is present in the frequency range extending from 0.4 to 0.6 MHz, and, even though this noise is 100 times greater than the R-wave signal, it is not apparent in the lower trace.

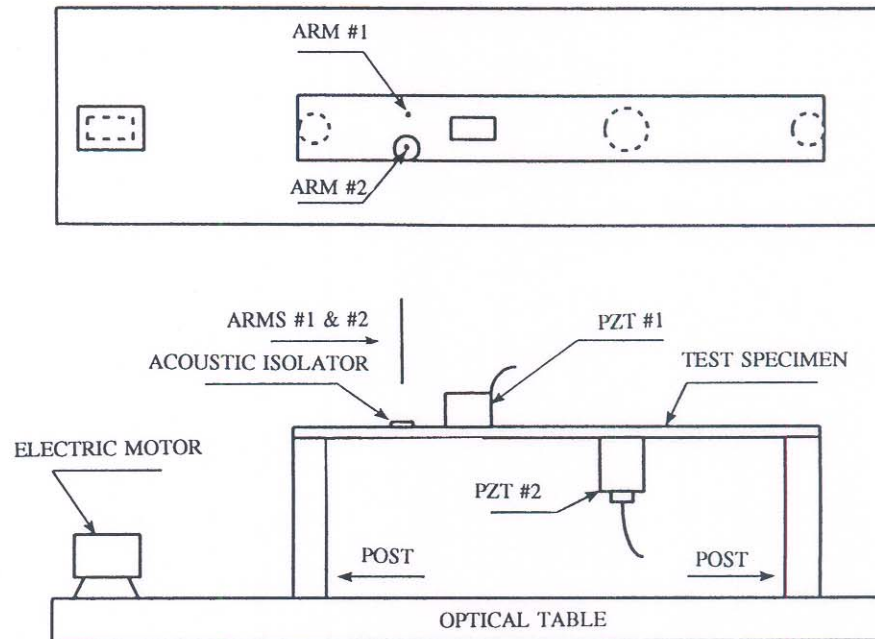


Fig. 6. The experimental setup used to acquire an R-wave in the presence of random noise. Arm #1 is positioned directly over the surface of the aluminum specimen while arm #2 is positioned over an acoustic isolator. Random noise is generated using an electric motor equipped with a rotating eccentric cam.

Extraction of an R-Wave from Noise of Similar Frequency

The noise produced by the motor described in the previous section is of relatively low frequency compared to that of the Rayleigh wave, so much so that, even if noise were present, there would be little effect on the frequency content of the Rayleigh wave. In this case, noise removal simply stabilizes the baseline of the DOI. However, in many practical applications involving the interaction of more complex structures, noise may occur at the same frequency as the Rayleigh wave; in this case, the ultrasonic signal would become contaminated. The following test demonstrates that the DOI is capable of removing noise at the same frequency of the Rayleigh wave.

Figure 8 shows a setup in which a Rayleigh wave is generated using the 2.25-MHz transducer labeled as #1. Noise is generated at the same frequency by using a similar transducer without the wedge required for R-wave generation (transducer #2). Both transducers are connected to the same pulse generator, so that the Rayleigh wave and the noise are generated at the same time. By doing so, only one external trigger is required.

One arm of the DOI is positioned over the upper surface of the specimen while the other is positioned above an adjacent acoustic isolator. Both optrodes are located at a distance of 20.5 mm from transducer #1.

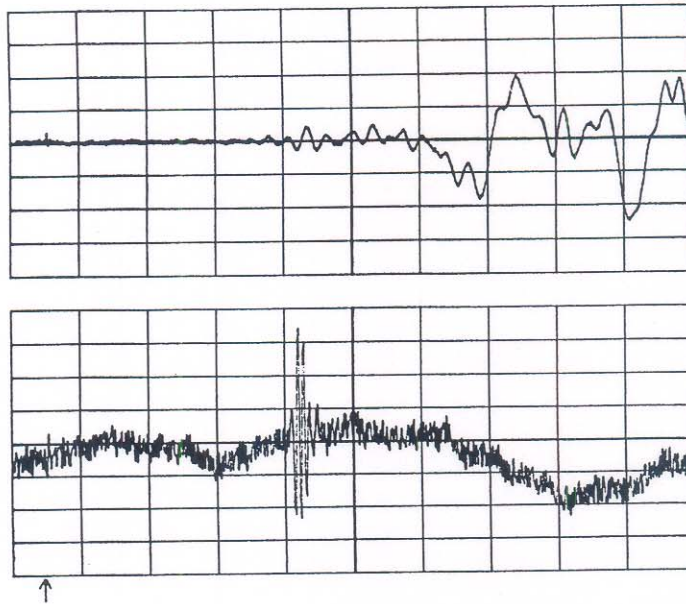


Fig. 7. Results obtained from the test setup shown in Fig. 7. The upper trace shows the noise detected by a 0.5-MHz transducer while the lower trace shows the R-wave detected by the DOI. The vertical gains on the upper and lower traces are 5 and 50 mV/div, respectively; the horizontal gain on each trace is 5 μ s/div.

To fully meet the objective of the test, the noise from transducer #2 must arrive at the DOI at the same time as the Rayleigh wave. Since the waves to which the noise may be attributed travel through aluminum at a velocity of 6.32 mm/ μ s, transducer #2 should be placed 107 mm away from the DOI. Also, because the DOI can only filter noise up to 37.7 KHz, transducer #2 needs to be strategically located so that the distances from the noise source to both arms of the DOI are equal. In an initial attempt to satisfy these criteria, the transducer was placed on the lower surface of the specimen along the longitudinal center line. When this was done, however, the noise level was found to be very low, so the transducer was moved closer to the DOI. In this case, the noise arrives at the DOI before the Rayleigh wave. Fortunately, however, the pulse fed to transducer #2 causes the crystal to oscillate for a time duration of 40–50 μ s, so that noise exists when the Rayleigh wave arrives.

Figure 9 shows the results obtained from the test. The feedback from transducer #2 is shown in the upper trace while the signal from the DOI is displayed in the lower; both traces were recorded 6.64 μ s prior to the recordings shown. The Rayleigh wave produced by transducer #1 and contained in the lower trace can be observed at the expected arrival time of 17.6 μ s (6.64 μ s prior to, plus 11 μ s on, the recordings). Figure 10 shows the results obtained when arm #2 was removed and immersed in an index matching fluid; in this case, the R-wave is contaminated with noise. Because the crystal in transducer

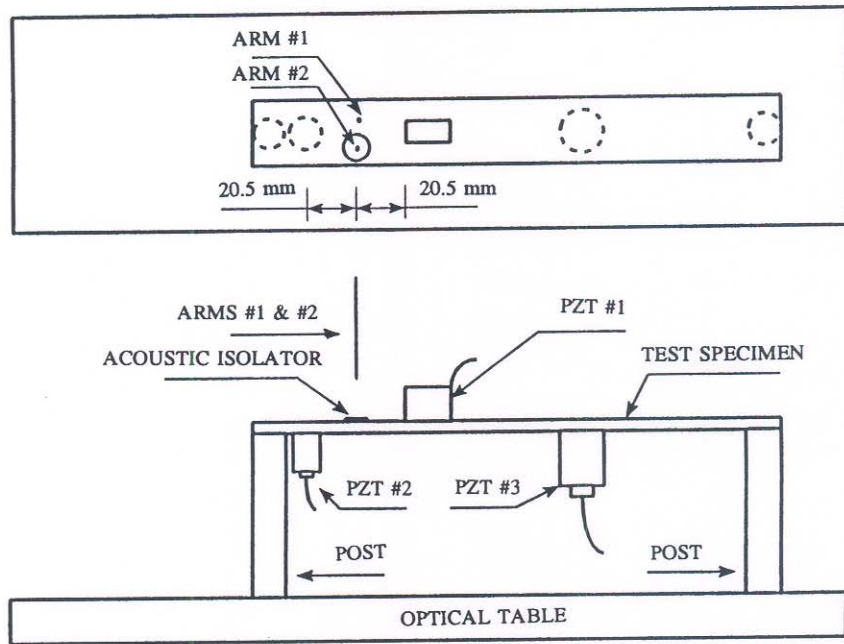


Fig. 8. The experimental setup used to acquire an R-wave in the presence of noise at the same frequency.

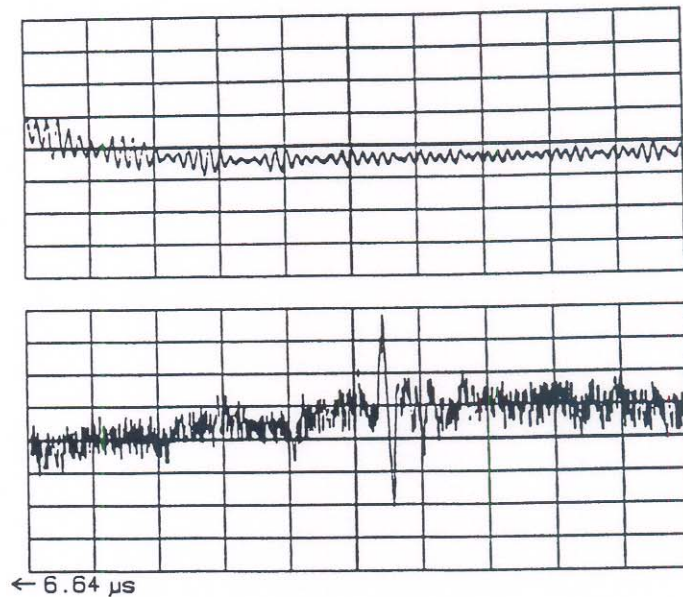


Fig. 9. Results obtained from the test setup shown in Fig. 9. The upper trace shows the feedback from the pulse generator while the lower trace shows the R-wave detected by the DOI. The vertical gains on the upper and lower traces are 50 mV/div; the horizontal gain on each trace is 2 $\mu\text{s}/\text{div}$.

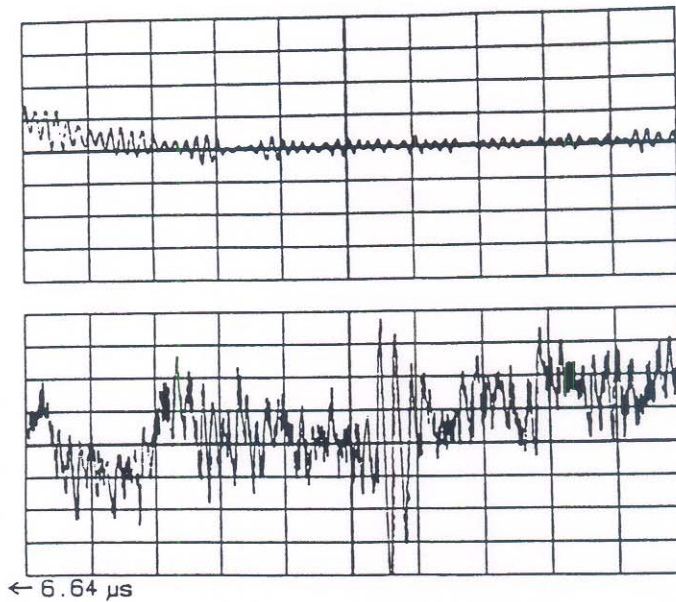


Fig. 10. Results obtained from the test setup shown in Fig. 9 with arm #2 immersed in an index matching fluid. The upper trace shows the feedback from the pulse generator while the lower trace shows the contaminated R-wave detected by the partially configured DOI. The vertical gains on the upper and lower traces are 50 mV/div; the horizontal gain on each trace is 2 μ s/div.

#2 continuously oscillates during the recording period, the noise is observed throughout the entire trace.

Conclusions

It has been shown that a differential optical interferometer (DOI) can be configured to detect R-waves in the presence of random noise which may be at a level that is substantially greater than, and at the same frequency as, that of the acoustic signal. The device has the potential to allow members of the ultrasonic community to look beyond what was previously considered an impenetrable noise barrier.

The advantages of the DOI are that it is compact, light-weight, and sensitive to all possible ultrasonic frequencies; the optical components used in its construction are rugged, corrosion-resistant, and insensitive to electromagnetic noise. In addition, measurements are noncontact and nondestructive.

Acknowledgments. This work was supported by the Consortium for Holography, Applied Mechanics and Photonics at the University of Alabama in Huntsville. The authors would like to thank Dr. Gary Workman and Mr. James Walker for their assistance in procuring some of the equipment used for the research and Ms. Yue-Hong Song for building a portion of the electronic circuitry.

References

1. B. A. Auld. *Rayleigh Wave Theory and Application*, Springer-Verlag, New York (1985).
2. I. G. Scott. *Basic Acoustic Emission*, Nondestructive Testing Monographs and Tracts, Vol. 6, p. 45, (1991).
3. M. G. Silk, *Ultrasonic Transducers for NDT*, Adam Hilger Ltd., Bristol (1984).
4. R. O. Cook and C. W. Hamm. *Appl. Opt.* **18**(19):3230 (1979).
5. H. R. Gallantree. *Marconi Rev.* **XLV**:49 (1982).
6. J. P. Monchalin. *IEEE Trans. Ultrason., Ferroelect. Freq. Contr.* **UFFC-33**(5):485 (1986).
7. T. D. Dudderar, B. R. Peters, and J. A. Gilbert. *IEEE Ultrasonics Symp.*, Oct. 3-6 (1989).
8. K. A. Murphy, M. F. Gunther, R. O. Claus, T. A. Tran, and M. S. Miller. *SPIE Smart Sensing, Process. and Instrument.* **1918**:110 (1993).
9. R. McBride, T. A. Carolan, J. S. Barton, S. J. Wilcox, W. K. D. Borthwick, and J. D. C. Jones, *Meas. Sci. Technol.* **4**:1122 (1993).